JOURNAL OF VIROLOGY, Dec. 2000, p. 11832–11840 Vol. 74, No. 24
0022-538X/00/$04.00+0


# Pathogenesis of Herpes Simplex Virus Type 1-Induced Corneal Inflammation in Perforin-Deficient Mice

EDDIE CHANG,[1] LAURENCE GALLE,[2] DAVID MAGGS,[2] D. MARK ESTES,[1,3] AND WILLIAM J. MITCHELL[1,3]*

*Department of Molecular Microbiology-Immunology, School of Medicine,[1] and Departments of Veterinary Medicine and Surgery[2] and Veterinary Pathobiology,[3] College of Veterinary Medicine, University of Missouri, Columbia, Missouri 65211*

Received 19 June 2000/Accepted 14 September 2000

**Herpetic stromal keratitis (HSK) is an inflammatory disease of the cornea that often results in blindness. It is mediated by a host immune response which is triggered by herpes simplex virus (HSV) infection. Immune effector mechanisms are hypothesized to be important in disease development. We investigated, in a mouse model, whether perforin-dependent cytotoxicity is an important effector mechanism in the production of HSK. Wild-type (C57BL/6) and perforin-deficient (PKO) mice were infected intracorneally with HSV-1 strain F. Clinical disease and histologic lesions of the cornea at 23 days postinfection (p.i.) were significantly less severe in HSV-1-infected PKO mice than in infected wild-type mice. mRNA for the chemokine macrophage inflammatory protein 1α (MIP-1α) was detected by reverse transcription-PCR in the corneas of infected wild-type mice but not in the corneas of infected PKO mice at 23 days p.i. Adoptive transfer of wild-type HSV-1 immune T-cell-enriched splenocytes into HSV-1-infected PKO mice restored the disease phenotype which was seen in infected wild-type mice. In contrast, mice carrying a null-function mutation in the Fas ligand, which is involved in an alternative cytotoxic mechanism, developed clinical disease and histologic lesions which were comparable to those in wild-type mice. Viral clearance from the eyes of PKO mice was not impaired. There was no significant difference between the infectious viral titers isolated from the eyes of PKO and wild-type mice. Our findings show that perforin is important in the pathogenesis of HSK.**

Herpetic stromal keratitis (HSK) is a chronic inflammation of the cornea which is a consequence of infection by herpes simplex virus (HSV). It is the main nontraumatic cause of corneal blindness in people in developed countries (54). HSV-1-induced corneal inflammation in the mouse model is an immunopathological condition mediated by T lymphocytes (11, 20–22, 38, 48, 49, 54). T-cell-deficient mice, such as athymic nude mice, *scid* mice, or thymectomized mice, do not develop keratitis following intracorneal infection with HSV-1. However, these mice develop HSK upon intracorneal HSV-1 infection if they have previously received an adoptive transfer of HSV-1 immune T lymphocytes (3, 11, 12, 21, 37, 43, 58).

The main effector mechanisms mediated by T lymphocytes are the secretion of soluble factors such as cytokines and chemokines and the lysis of target cells. Cytokines, such as gamma interferon, have been proposed as mediators of HSK (2, 20, 24). However, studies of gamma interferon knockout mice failed to demonstrate a role for gamma interferon in the pathogenesis of HSV-induced stromal keratitis (5). Chemokines have also been postulated to be involved in the development of HSK (55, 57, 59). There is evidence that macrophage inflammatory protein 1α (MIP-1α), a beta chemokine involved in lymphocyte recruitment, plays a role in the development of HSK (60).

Immune cytotoxic effector mechanisms play a role in the development of many immune-mediated disorders. The two main cytotoxic effector mechanisms are perforin-mediated cytotoxicity and the Fas-Fas ligand (FasL) pathway (27, 28, 30, 35, 53). In the Fas-FasL pathway, FasL expressed on the surface of cytotoxic lymphocytes engages the Fas receptor expressed on target cells. This interaction triggers a cascade of signals, which results in apoptosis of the target cells. In the perforin pathway, effector cells such as cytotoxic T lymphocytes (CTL) and natural killer (NK) cells secrete granules containing perforin, which polymerize to form channels in the plasma membrane of target cells. The polyperforin channels lead to the death of target cells by providing a portal of entry of apoptosis-mediating granzymes into the target cells.

The Fas-FasL pathway has been implicated in the pathogenesis of experimental autoimmune encephalitis (50, 62) and diabetes (1). The importance of perforin-mediated cytotoxicity has been demonstrated for the development of lymphocytic choriomeningitis virus-induced immunopathology (27, 28, 48), mouse hepatitis virus-induced encephalomyelitis (34), and coxsackievirus B3-induced myocarditis (16). A recent study demonstrated that both cytotoxic mechanisms were important in the development of contact hypersensitivity (29). A role for immune cell-mediated cytotoxicity in the pathogenesis of HSK has been suggested based on the findings that cytotoxic T lymphocytes were generated in mice following corneal infection with HSV-1 (10, 11, 21, 23, 25, 31) and in human patients (71, 72). Another study showing that depletion of cytotoxic NK cells resulted in reduced susceptibility to HSK (6) is also consistent with a role for immune-mediated cytotoxicity in HSK. However, the role of cytotoxic effector mechanisms in the pathogenesis of HSK has not been investigated in detail.

In this study, we examined the role of perforin-mediated cytotoxicity in the pathogenesis of HSK by studying the development of HSV-1-induced corneal inflammation in mice deficient in perforin. Compared to wild-type mice, the severity of the clinical signs of HSK was significantly reduced in perforin-deficient (PKO) mice. Histologic examination showed that inflammatory lesions of the cornea following intracorneal infec-

* Corresponding author. Mailing address: Department of Veterinary Pathobiology, 201 Connaway Hall, University of Missouri, Columbia, MO 65211. Phone: (573) 882-5421. Fax: (573) 884-5414. E-mail: MitchellWJ@missouri.edu.

tion with HSV-1 strain F were less severe in PKO mice than in wild-type mice. mRNA for the chemokine MIP-1α was detected in the corneas of wild-type but not PKO mice at 23 days postinfection (p.i.). PKO mice which received HSV-1 immune effector cells from wild-type mice developed HSK of similar severity to that seen in wild-type mice following corneal inoculation with HSV-1. There were no differences in the ability of wild-type and PKO mice to clear HSV-1 from the eye following intracorneal inoculation. In contrast to the above findings, the severity of HSK was not reduced in *gld* mice, which cannot mediate cytotoxicity via the Fas-FasL mechanism (*gld* mice have a null-function mutation in the *fasL* gene). These findings illustrate that perforin-mediated cytotoxicity is an immune effector mechanism that plays a key role in the development of HSK.

## MATERIALS AND METHODS

**Animals.** Mice containing a targeted disruption in the perforin gene (C57BL/6pfp$^{tm1sdz}$, perforin-deficient [PKO] mice) and mice carrying a null-function mutation of the *fasL* gene (B6Smn.C3HFasL$^{gld}$, *gld* mice; backcrossed 16 times to C57BL/6 mice [Technical Support, Jackson Laboratory, personal communication]), and wild-type C57BL/6 controls (B6, congenic with FasL mutant mice) were purchased from Jackson Laboratory (Bar Harbor, Maine). The mice were bred and maintained under specific-pathogen-free conditions in filter top cages at the animal facility of the University of Missouri. All experiments were done in accordance with a protocol approved by the Animal Care and Use Committee of the University of Missouri. Both male and female mutant mice and their wild-type counterparts were between 8 and 9 weeks of age when used in the experiments.

**Animal infection and clinical observations.** HSV-1 strain F, a viral strain which induces keratitis in mice (42), was used in all experiments. Virus stocks were grown and subjected to titer determination on Vero cells (41), and corneal infection of mice was performed as previously described (36). The mice were anesthetized with methoxyflurane, and the cornea of each eye was scarified with a 26-gauge needle. Then $10^7$ PFU of HSV-1F in 5 μl of Dulbecco's modified Eagle's medium (DMEM) containing 5% fetal calf serum was applied to the corneal surface of each eye, and the eyelids were massaged. Mock-infected mice received 5 μl of DMEM containing 5% fetal calf serum.

Eyes were examined for corneal opacification and neovascularization by using slit lamp biomicroscopy. Examiners were masked regarding the genotype and viral infection status of each mouse. Corneal opacification and neovascularization were graded on a scale from 0 through 4 using a previously published scoring system with minor modifications (7, 18). Corneal opacification was scored as follows: 0, normal/absent; 1, mild opacification, iris detail visible; 2, iris detail obscured; 3, cornea totally opaque; 4, cornea perforated. Neovascularization was scored as follows: 0, normal/absent; 1, less than 25% of cornea vascularized; 2, 25 to 50% of cornea vascularized; 3, 50 to 75% of cornea vascularized; 4, greater than 75% of cornea vascularized. Mean disease scores were calculated for each eye on each day of observation by averaging the sum of the opacification and neovascularization scores. The clinical lesion data presented in Fig. 1A were pooled from two separate experiments. In the first experiment, four PKO and four wild-type mice were infected with HSV-1F and one PKO and one wild-type mouse were mock infected. In the second experiment, six PKO and six wild-type mice were infected with virus and two PKO and two wild-type mice were mock infected. The data in Fig. 1B were from one experiment using seven infected wild-type mice, six infected *gld* mice, and one mock-infected mouse from each genotype. For all clinical lesion experiments not involving adoptive transfer, HSV-1-infected and mock-infected wild-type and mutant (PKO or *gld*) mice were examined for clinical disease at 5, 11, 18, and 23 days p.i. In the two experiments in which PKO mice received adoptive transfers of wild-type spleen cells (see, "Adoptive transfer studies" below), the mice were examined for clinical disease 5, 8, 11, 14, 18, 20, and 23 days p.i.

**Histologic analysis.** At 23 days after infection with HSV-1, 10 wild-type mice and 10 PKO mice were sacrificed and both eyes were removed from each mouse. The eyes were fixed overnight in 4% paraformaldehyde in phosphate-buffered saline (PBS), followed by 70% ethanol. Fixed eyes were embedded in paraffin, and 7-μm serial sections were made. Care was taken to ensure that all eyes in the same block were embedded at the same level. Sections 25, 45, and 65 of each eye (with section 1 beginning at approximately 70 μm from the corneoscleral limbus) were stained with hematoxylin and eosin and examined by light microscopy to grade inflammatory lesions and to measure corneal thickness. The examiner was masked regarding the genotype and virus infection status of each mouse when conducting the histologic analysis. A histologic lesion score was assigned based on the extent of inflammatory-cell infiltration and vascularization present within the cornea. Twelve random 40× fields which included corneal stroma were examined from each corneal section to assess the extent of vascularization and inflammatory-cell infiltration. An inflammatory-cell infiltration score and a vascularization score were assigned to each field. Inflammatory-cell infiltration scores were assigned as follows: 0, no cellular infiltration; 1, cellular infiltrate occupied <25% of the field; 2, cellular infiltrate occupied 25 to 50% of the field; 3, cellular infiltrate occupied 50 to 75% of the field; 4, cellular infiltrate occupied >75% of the field. Vascularization scores were assigned as follows: 0, no vascularization; 1, vascularization occupied <25% of the field; 2, vascularization occupied 25 to 50% of the field; 3, vascularization occupied 50 to 75% of the field; 4, vascularization occupied >75% of the field. The inflammatory-cell infiltration score and vascularization score of all fields from each cornea (total of 36 fields for all three sections of each cornea) were then added and averaged to obtain the histologic lesion score presented in the text and Fig. 3. Each micrograph in Fig. 2A to D was taken from section 25 of a representative mouse cornea, and the micrograph in Fig. 2E was taken from section 45 of a representative mouse cornea.

Corneal thickness was measured at the thickest point of the cornea by using a stage micrometer. Sections 25, 45, and 65 of each eye were measured. Corneal thickness measurements from the three sections for each eye were averaged to obtain a value for each eye. A total of 19 eyes from infected wild-type mice and 18 eyes from infected PKO mice were examined in the histologic analysis (three eye samples were lost prior to processing and were excluded from the study). The data for the histologic analysis described in this section were pooled from two separate experiments. Four PKO and four wild-type mice were infected with HSV-1F, and one mouse of each genotype was mock infected in one experiment. In another experiment, six PKO and six wild-type mice were infected with virus and two mice of each genotype were mock infected.

The eyes of HSV-1-inoculated FasL mutant (*gld*) mice were evaluated histologically. The eyes of six *gld* mice and seven wild-type mice 23 days after infection with HSV-1 were fixed, processed, and stained as described above. Sections were examined by light microscopy.

**Preparation of RNA, RT, and PCR.** Two separate experiments were performed. In each experiment, corneas were harvested from three HSV-1-infected wild-type and three HSV-1-infected PKO mice 23 days p.i. Samples were also harvested from one mock-infected mouse of each gentoype. Both corneas from each mouse were pooled and processed individually. Total cellular RNA was isolated from the pooled corneas of each mouse using the RNAeasy Mini Kit as specified by the manufacturer (Qiagen, Santa Clarita, Calif.). A 200-ng portion of corneal RNA from each mouse was reverse transcribed into cDNA using the following reaction mixture: 5 mM $MgCl_2$, 50 mM KCl, 10 mM Tris-HCl (pH 8.3), 1 mM each dGTP, dATP, dCTP, and dTTP, 2.5 U of murine leukemia virus MuLV reverse transcriptase, 1 U of RNase inhibitor, and 2.5 μM of random hexamers. Reverse transcription (RT) was performed for 15 min at 42°C followed by 5 min at 99°C and 5 min at 5°C.

To normalize the cDNA samples, PCR for hypoxanthine phosphoriboxyltransferase (HPRT) cDNA was performed on each of the test samples. A 3-μl volume of cDNA from each mouse was added to the following reaction mixture: 3.8 mM $MgCl_2$, 50 mM KCl, 10 mM Tris-HCl (pH 8.3), 1 mM each dGTP, dATP, dCTP, and dTTP, 50 ng each of sense (5′GTTGGATACAGGCCAGACTTTGTTG 3′) and antisense (5′GATTCAACTTGCGCTCATCTTAGGC3′) HPRT primers (56), and 2.5 U of *Taq* polymerase in a final reaction volume of 50 μl. PCR was run at 94°C for 2 min, followed by 32 cycles at 94°C for 45 s, 60°C for 1 min, and 72°C for 1.5 min, with 1 extension cycle at 72°C for 7 min (56). The 182-bp HPRT PCR product for each sample was detected by agarose gel electrophoresis and ethidium bromide staining. Gels were photographed under UV light, and the HPRT PCR product bands were quantitated using a DC120 Image Analyzer (Kodak, Rochester, N.Y.). The cDNA samples were adjusted so that an amount of cDNA for each sample was used that yielded equal amounts of HPRT amplification product.

For MIP-1α amplification, normalized cDNA from each mouse was amplified by PCR for 32 cycles as described above. The PCR mixture was as described above, except that 2 mM $MgCl_2$ and 50 ng each of sense (5′CAGCGAGTACC AGTCCCTTTT3′) and antisense (5′CCTCGCTGCCTCCAAGA3′) MIP-1α primers (9) were used. The 364-bp MIP-1α PCR product for each sample was detected and photographed as described above.

**Adoptive-transfer studies.** Donor cells (T-cell-enriched splenocytes) were prepared from wild-type mice using a previously published method (52). Briefly, wild-type mice between 8 and 9 weeks of age were infected intracorneally with $10^7$ PFU of HSV-1F per eye and sacrificed 23 days p.i. Their spleens were removed and macerated in sterile RPMI 1640 medium (containing 5% fetal calf serum) with sterile frosted slides. The cell suspension was washed twice in sterile Hanks balanced salt solution (HBSS) and resuspended at $10^7$ cells/ml in panning solution (HBSS [pH 7.4] containing 3% bovine serum albumin [BSA], 50 μl of gentamicin per ml, 10 mM Tris-HCl, 2.5 μM $CaCl_2$, and 0.9 μM $MgCl_2$). B lymphocytes were allowed to adhere to plastic at room temperature for 1 h. B cells were further depleted from the nonadherent cells by the use of anti-mouse immunoglobulin G and magnetic beads. Briefly, cells were washed in 0.1% BSA in HBSS and incubated on ice for 20 min in biotin-labeled anti-mouse IgG at a final concentration of 50 μg/ml. The cells were washed and resuspended in 0.1% BSA in HBSS, and strepavidin-coated magnetic beads were added (3:1 bead-to-cell ratio). The cells were incubated at 4°C for 10 min on a rotary shaker, and beads were removed by applying a magnet to the cell suspension. The cells in the liquid phase containing T-cell-enriched splenocytes were washed and resuspended in sterile 0.1% BSA in PBS at a concentration of $10^8$ cells/ml. For

adoptive transfer, $4 \times 10^7$ T-cell-enriched donor splenocytes (0.4 ml of cell suspension) were injected by the intraperitoneal route into each 8- to 9-week-old PKO (recipient) mouse. Control recipient mice were injected intraperitoneally with 0.4 ml of sterile 0.1% BSA in PBS. All recipient mice were infected intracorneally with $10^7$ PFU of HSV-1F per eye as described above immediately after receiving donor cells or BSA-PBS. Recipient mice were evaluated clinically throughout the course of infection as described above. The data presented in Fig. 6 were combined from two experiments. In the first experiment, a total of eight PKO recipients were used; four received T-cell-enriched splenocytes and four received PBS only. In the second experiment, 10 PKO recipient mice were used; 5 received T-cell-enriched splenocytes, and 5 received PBS only.

At 23 days p.i., the eyes of five virus-infected PKO mice which received adoptive transfer of splenocytes and five virus-infected PKO mice which received only PBS were fixed, processed, and stained as described previously. The sections were examined by light microscopy. The micrograph in Fig. 2F was taken from a representative cornea from a PKO mouse that received wild-type HSV-1 immune splenocytes.

**Virus titer determination.** For the experiment in Fig. 5A, eyes were removed from HSV-1-infected PKO and wild-type mice 5, 11, and 23 days p.i. The data were pooled from two separate experiments. Three wild-type and three PKO mice were used at each time point in the first experiment, and six mice from each group were used at each time point in the second experiment. For the one experiment in which viral clearance was examined during acute HSV-1 infection (see Fig. 5B), eyes were removed from four infected wild-type and PKO mice at 1, 3, 5, 8, and 11 days p.i. Each eye was placed in 1 ml of DMEM containing 5% fetal calf serum and stored at −70°C until assayed. For virus titer determination, whole eyes were thawed and homogenates were prepared from each eye using a tissue homogenizer. Whole-eye homogenates were subjected to infectious-virus titer determination on Vero cells overlaid with methylcellulose in a standard plaque assay (42). Only seven eyes from infected wild-type mice 3 days p.i. (see Fig. 5B) were examined, since one eye from this group was lost prior to sample processing.

**Statistics.** The Mann-Whitney rank-sum test was used to determine significant differences in the clinical and histologic disease. Student's *t* test was used to determine significant differences in the corneal thickness and virus titers. The level of confidence at which differences between experimental groups were judged to be significant was $P < 0.05$.

## RESULTS

**Mice deficient in perforin had less severe clinical lesions of keratitis following corneal infection with HSV-1F.** Perforin-deficient (PKO) mice and wild-type control (C57BL/6) mice were infected with HSV-1 strain F ($10^7$ PFU per eye) and examined as described in Materials and Methods. The examination time points included the period of acute viral replication through the peak clinical phase of herpetic stromal keratitis (2, 42). No significant progression in disease severity in the clinical phase after 23 days p.i. was observed in preliminary studies (data not shown). At 5 days p.i., both groups of mice showed mild clinical disease, with mean disease scores of 1 for both groups of mice (Fig. 1A). In the wild-type mice, clinical disease was progressive and the mean disease score increased from 1.4 at 11 days p.i. to a peak of 2.4 at 18 days p.i. and remained at 2.3 by 23 days p.i. (Fig. 1A). In contrast, clinical disease in PKO mice did not progress and the mean disease scores following HSV-1 infection were 0.55, 0.45, and 0.45, at 11, 18, and 23 days p.i., respectively (Fig. 1A). The mean clinical disease scores of HSV-1-infected PKO mice were significantly lower ($p < 0.05$) than mean disease scores of HSV-1-infected wild-type mice at 11, 18, and 23 days p.i. (Fig. 1A).

We tested a second pathway for target cell killing by cytotoxic lymphocytes to determine whether the disease phenotype seen in HSV-1-infected PKO mice was specific to perforin-mediated cytotoxicity. We examined whether a deficiency in the FasL pathway of CTL-mediated cytotoxicity affected the severity of herpetic stromal keratitis. Mice carrying a null-function mutation in *fasL* (*gld* mice) were infected with HSV-1F ($10^7$ PFU per eye) and examined using the same method and design as described above. HSV-1-infected wild-type and *gld* mice showed gradually worsening clinical disease during the onset phase and for the duration of the experiment (Fig. 1B). The mean disease scores were not significantly different between HSV-1-infected *gld* and wild-type mice at any time point (Fig. 1B). The progress of clinical disease severity in wild-type and *gld* mice paralleled that seen in other studies (3, 13, 37, 39, 42).

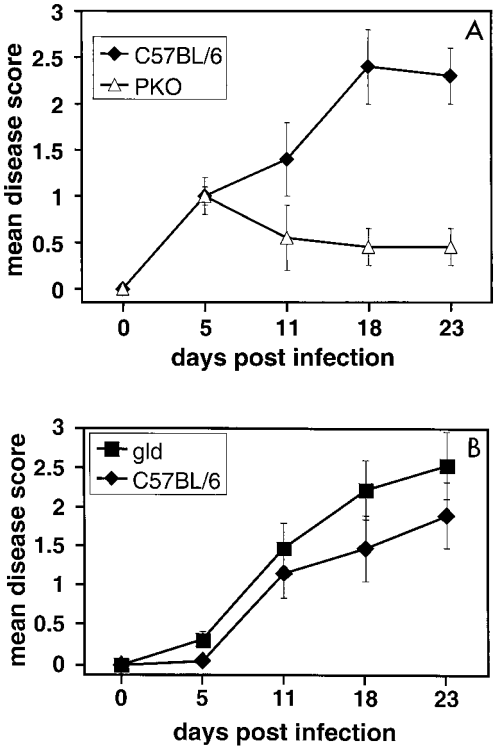


FIG. 1. Mean clinical disease scores for keratitis in PKO, *gld*, and wild-type mice infected with HSV-1F. (A) Mean clinical disease scores for keratitis in HSV-1-infected PKO and wild-type (C57BL/6) mice; the difference in mean disease scores between PKO and wild-type mice was statistically significant at 11, 18, and 23 days p.i. ($P < 0.05$). (B) Mean clinical disease scores for keratitis in *gld* mice carrying a null-function mutation in Fas ligand and wild-type mice; the difference in the mean disease scores between *gld* and wild-type mice was not statistically significant. (A) A total of 10 PKO mice and 10 age-matched wild-type mice were infected intracorneally with HSV-1 ($10^7$ PFU/eye) and examined for corneal opacification and neovascularization at the time points indicated. Mean disease scores were calculated as described in Materials and Methods. (B) Same as in panel A, except that six HSV-1-infected *gld* mice and seven virus-infected wild-type mice were used. No clinical disease was detected in mock-infected mice (wild-type, PKO, or *gld*) at any time point. Bars indicate the standard error of the mean disease score.

Mock-infected wild-type, PKO, and *gld* mice did not develop clinical disease during the course of the experiment (mean clinical disease score = 0 at all time points examined). There were no deaths of any mice in the wild-type, PKO, or *gld* groups which were infected with $10^7$ PFU of HSV-1F by the corneal route.

**Mice deficient in perforin had less severe histopathologic lesions of keratitis than wild-type mice following infection with HSV-1.** Extensive inflammatory-cell infiltration was present in the corneas of HSV-1-infected wild-type mice at 23 days p.i. (Fig. 2A). The inflammation consisted of neutrophils, macrophages, and lymphocytes, with neutrophils being the most prominent population present in the lesions (Fig. 2B). Extensive vascularization was also present in the corneal stroma of infected wild-type mice (Fig. 2A and B). Epithelial necrosis was present in many corneas which had large amounts of inflammation. The increased inflammation resulted in increased corneal thickness at 23 days p.i. in the infected wild-type mice compared to the mock-infected wild-type mice (Figs. 2A and

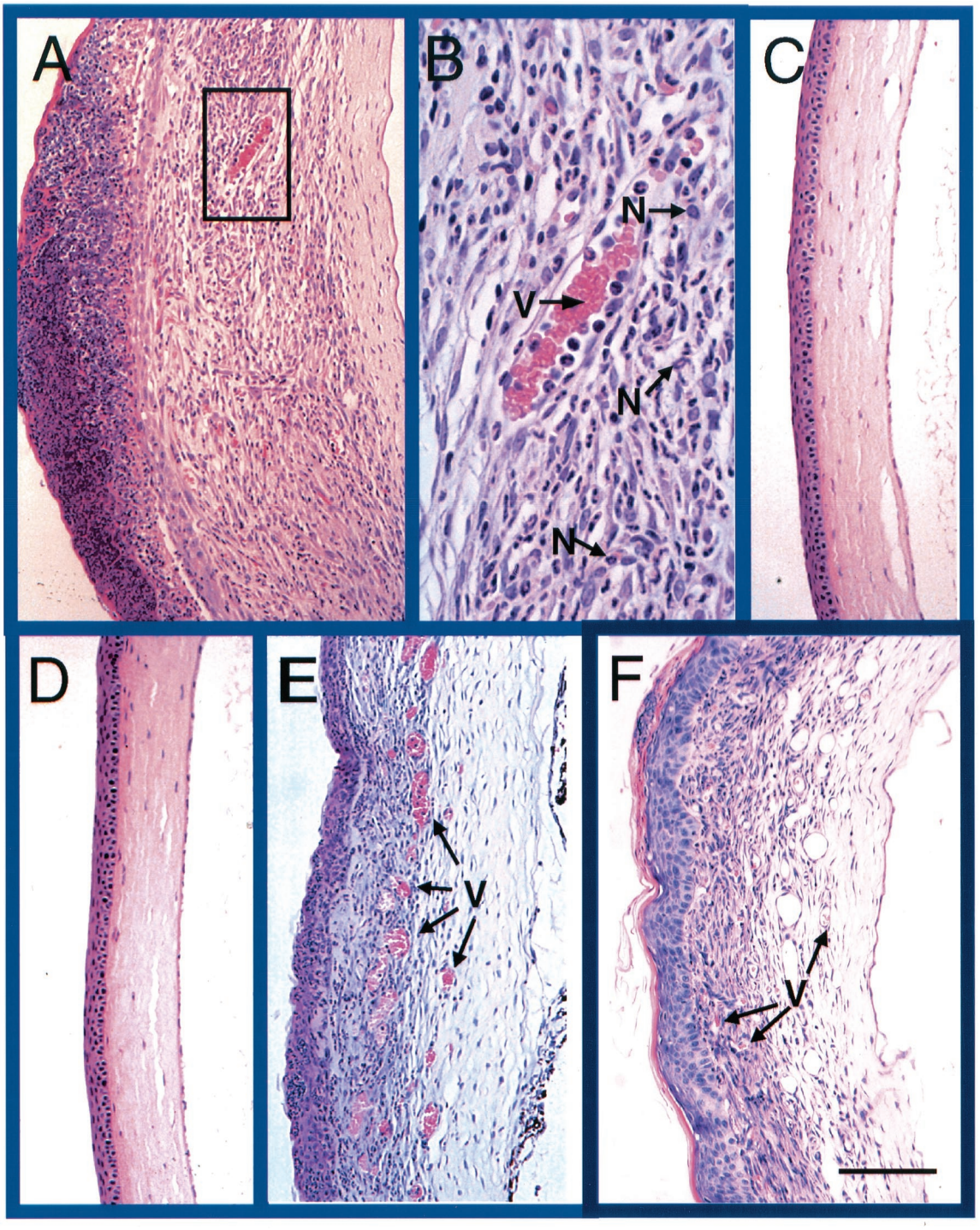


FIG. 2. Hematoxylin-and-eosin-stained sections from PKO, reconstituted PKO, *gld*, and wild-type mice 23 days after infection with HSV-1F. (A) Cornea of infected wild-type mouse, showing extensive inflammation. (B) Higher magnification of the demarcated area in panel A. Note the large vessel (V) and inflammatory-cell infiltrate present in the corneal lesion, with neutrophils (N) being the most prominent cell type present. (C) Cornea of infected PKO mouse showing little inflammation. (D) Cornea of mock-infected wild-type mouse. (E) Cornea of infected *gld* mouse. (F) Cornea of PKO mouse reconstituted with wild-type HSV-1 immune T-cell-enriched splenocytes. Note the inflammation and vascularization (indicated by V) in panels E and F. Bar, 100 μm (A and C to F) and 35 μm (B).

D; also see Fig. 4). The histologic lesions observed in HSV-1-infected FasL mutant (*gld*) mice (Fig. 2E) were similar to those seen in wild-type mice.

In contrast, the corneas of infected PKO mice at 23 days p.i. showed less prominent inflammatory cell infiltration than did those of infected wild-type mice (Fig. 2A and C and 3). In general, inflammatory cells were either scattered throughout the stroma, present only in the peripheral limbal region of the cornea, or absent in PKO mice. Of 18 PKO mouse corneas at 23 days p.i., 2 had significant inflammatory infiltrate. The corneas of HSV-1-infected PKO mice had little vascularization or epithelial necrosis. Overall, the corneas of infected PKO mice

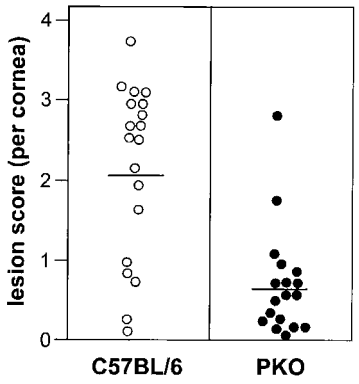


FIG. 3. Histologic lesion scores for corneas in PKO and wild-type mice 23 days after infection with HSV-1F. A histologic lesion score was assigned as described in the text for each eye based on the extent of cellular infiltration and vascularization. The mean lesion score was 0.7 for PKO mice and 2.1 for wild-type (C57BL/6) mice ($P < 0.05$). Mean lesion scores are indicated by the horizontal bars. PKO mice and age-matched wild-type mice were infected intracorneally with $10^7$ PFU of HSV-1 per eye. Each circle in the figure represents the histologic lesion score for one eye.

at 23 days p.i. were more similar to mock-infected corneas than to infected corneas of wild-type mice (Fig. 2A, C, and D). Mock-infected wild-type, PKO, and *gld* mice had no histologic lesions at 23 days after mock infection.

HSV-1-infected corneas from wild-type and PKO mice at 23 days p.i. were assigned a histologic lesion score based on the criteria described in Materials and Methods. The distribution of histologic lesion scores for each cornea that was examined is shown in Fig. 3. The infected corneas of wild-type mice had higher lesion scores (mean, 2.1) than did infected corneas of PKO mice (mean, 0.7) (Fig. 3, horizontal bars). This difference in histologic lesion scores between infected corneas of wild-type and PKO mice was statistically significant ($P < 0.05$).

Differences in inflammation between corneas of HSV-1-infected PKO and wild-type mice resulted in significant differences in corneal thickness (Fig. 4). At 23 days p.i., the corneas

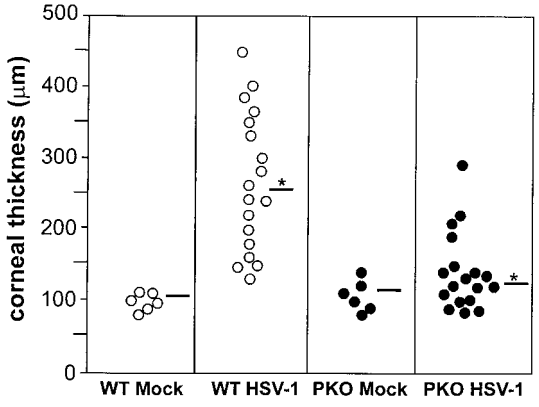


FIG. 4. Corneal thickness in HSV-1F-infected PKO and wild-type mice at 23 days p.i. PKO and wild-type mice were infected and eyes were processed as described in the text. The corneal thickness for each eye at the thickest point was measured using a stage micrometer. Sections 25, 45, and 65 of each eye were measured. The three values for each eye were averaged to obtain the data presented in this figure. Each circle represents the corneal thickness of one eye. The average corneal thickness for all eyes examined in each group is represented by the horizontal bars. The difference in corneal thickness between infected wild-type mice (WT HSV-1; mean, 255 μm) and infected PKO mice (PKO HSV-1; mean, 124 μm), indicated by the asterisk, was statistically significant ($P < 0.05$).

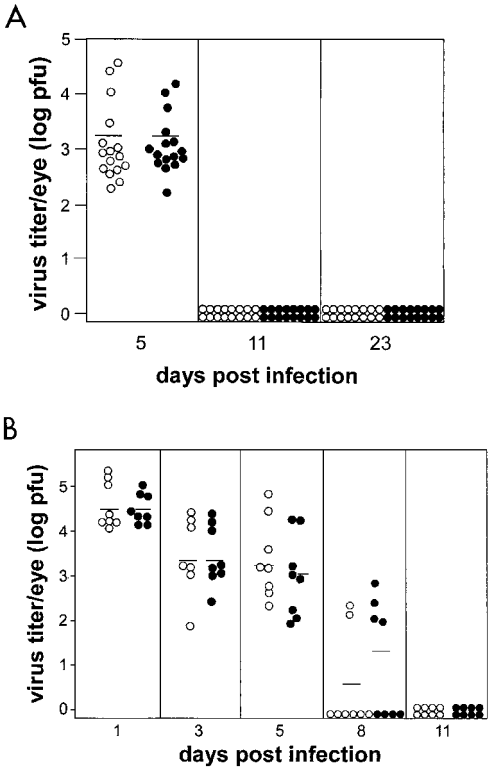


FIG. 5. Infectious virus titers recovered from the eyes of HSV-1F-infected PKO and wild-type mice. Mice were infected as indicated in Materials and Methods. (A) Three mice from each group were sacrificed at 5, 11 and 23 days p.i. in one experiment and five mice from each group were sacrificed at each time point in the second experiment. The results from the two experiments were pooled. (B) Four mice from each group were sacrificed at 1,3, 5, 8 and 11 days p.i. Viral titers were determined using a plaque assay. Open circles, virus titers isolated from each eye of infected wild-type (C57BL/6) mice; solid circles, virus titers isolated from each eye of infected PKO mice. Horizontal bars indicate the mean viral titer.

of HSV-1-infected wild-type mice had a mean thickness of 255 μm compared to 124 μm for those of HSV-1-infected PKO mice (Fig. 4, horizontal bars with asterisk, [$P < 0.05$]). The mean corneal thickness for mock-infected wild-type (105 μm) and PKO mice (113 μm) (Fig. 4, horizontal bars) were not statistically different from those of HSV-1-infected PKO mice.

**Clearance of HSV-1 from the eyes was not altered in PKO mice.** Perforin-mediated cytotoxicity is involved in the antiviral immune response and is important in the clearance of some viruses (27, 28, 35, 53, 63). In vitro studies have shown that HSV-1-specific CTL use perforin-dependent cytotoxicity to lyse virus-infected target cells (70–73). Therefore, it was of interest to examine whether viral clearance was impaired in PKO mice. Viral titers in the eyes of PKO mice were compared with those in wild-type mice at 5, 11, and 23 days p.i. Wild-type and PKO mice had comparable virus titers at 5 days p.i. However, no infectious virus could be isolated from the eyes of either group at 11 or 23 days p.i. (Fig. 5A). In a second experiment, we determined whether there was a difference in viral titers between wild-type and PKO mice during acute viral replication. We compared the viral titers in the eyes of infected wild-type and PKO mice at 1, 3, 5, 8, and 11 days p.i. and found no significant differences (Fig. 5B). Virus titers were reduced in both groups of mice by 8 days p.i., and virus could not be detected in either group of mice by 11 days p.i. (Fig. 5B).

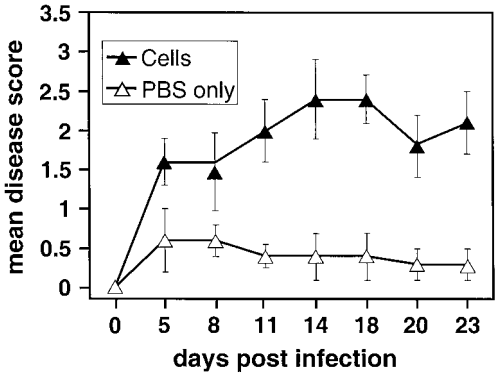


FIG. 6. Mean disease scores of HSV-1-infected PKO mice receiving adoptive transfer of HSV-1-immune splenocytes from wild-type mice. Nine PKO mice were given $4 \times 10^7$ T-cell-enriched splenocytes from infected wild-type donor mice. Nine PKO mice were given sterile PBS as control. All the mice were infected intracorneally with HSV-1F immediately after transfer, as described in the text. Mice were examined for corneal opacification and vascularization at the time points indicated, and mean disease scores were calculated. The difference in mean disease scores between the two groups of PKO recipient mice was statistically significant from 11 days p.i. onward ($P < 0.05$). Bars indicate the standard error of the mean disease score.

**T-cell-enriched splenocytes from HSV-1-infected wild-type mice were sufficient to restore keratitis of wild-type severity to PKO mice following infection with HSV-1.** We examined whether the decreased development of keratitis in PKO mice was specifically associated with perforin deficiency in the effector T cells that mediate the immunopathology. T-cell-enriched splenocytes from HSV-1-immune wild-type mice were adoptively transferred into PKO mice which were infected with HSV-1F. PKO mice were given $4 \times 10^7$ T-cell-enriched splenocytes from wild-type donor mice that had been infected with HSV-1 23 days before the transfer. The PKO recipient mice were then infected intracorneally with HSV-1 on the same day. Following HSV-1 infection, PKO mice that received splenocytes from HSV-1-immune wild-type mice developed progressive clinical disease which was comparable in kinetics and severity to that seen in infected wild-type mice (Fig. 1A and 6). The mean disease scores reached 2 at 11 days p.i., 2.4 at 18 days p.i., and 2.1 at 23 days p.i. (Fig. 6). In contrast, HSV-1-infected PKO recipient mice that did not receive HSV-1-immune splenocytes from wild-type donors had mean disease scores of 0.4, 0.4, and 0.3 at 11, l8, and 23 days p.i., respectively. The mean clinical disease scores were significantly greater in PKO mice receiving adoptive transfer than in sham-treated PKO mice from 11 days p.i. onward (Fig. 6; $P < 0.05$). At 23 days p.i., histologic lesions were present in the corneas of HSV-1-infected PKO mice which received HSV-1-immune splenocytes from wild-type mice. Lesions were characterized by the presence of inflammation and vascularization in the stroma and were similar to those seen in HSV-1-infected wild-type mice (Fig. 2A and F). The lesions were mild or absent in the corneas of virus-infected PKO mice which did not receive splenocytes from wild-type donors. In summary, adoptive transfer of HSV-1-immune T-cell-enriched spleen cells from wild-type mice was sufficient to restore HSK in PKO mice following HSV-1 infection.

**MIP-1α mRNA was detected in HSV-1-infected corneas of wild-type mice but not in HSV-1 infected corneas of PKO mice.** Elevated levels of MIP-1α mRNA and protein were previously demonstrated in the corneal lesions of HSK in a mouse model (57, 59, 60). The importance of this chemokine in lesion formation in previous studies was demonstrated by HSV-1 infection of MIP-1α-deficient mice; these mice developed less severe lesions than wild-type mice did (60). Therefore, it was of interest to determine whether the presence of MIP-1α in HSK was correlated with the presence of perforin and inflammatory cells. We examined whether the difference in corneal inflammation observed in HSV-1-infected wild-type and PKO mice would also be reflected by differences in the presence of MIP-1α mRNA in the cornea. As determined by RT-PCR, MIP-1α mRNA was readily detectable in the corneas of HSV-1-infected wild-type mice at 23 days p.i. (Fig. 7, lanes 1 to 3); however, MIP-1α mRNA was not detected in the corneas of HSV-1-infected PKO mice at 23 days p.i. (lanes 4 to 6). No MIP-1α mRNA could be detected in the corneas of mock-infected wild-type or PKO mice (lanes 7 and 8). All of the samples which were tested for MIP-1α contained equivalent amounts of cDNA as determined by HPRT amplification. MIP-1α primers yielded a 364-bp PCR product from cDNA (lanes 1 to 3). However, no PCR product of 1,000 bp was detected (a 1,000-bp fragment would have resulted if genomic DNA had been amplified using these primers). The experiment described above was repeated using three wild-type and three PKO mice infected with HSV-1. As in the first experiment (Fig. 7), MIP-1α mRNA was detected by RT-PCR in the corneas of all three HSV-1-infected wild-type mice but in none of the corneas of HSV-1-infected PKO mice (results not shown). All samples had equivalent amounts of HPRT mRNA as indicated by RT-PCR. PCR for MIP-1α was performed on aliquots of RNA (no reverse transcriptase was added) from the same corneas described above in the second experiment. No MIP-1α PCR product was detected in the absence of reverse transcriptase (results not shown). The absence of MIP-1α mRNA from the corneas of HSV-1-infected PKO mice is consistent with the relative absence of inflammatory cells from the corneas of infected PKO mice.

## DISCUSSION

Previous studies have shown that HSV-1-induced keratitis in the mouse model is an immunopathologic disease mediated by the effector functions of immune T cells (2, 11, 20, 24, 58). In this study we have used PKO mice to test the hypothesis that the perforin-mediated pathway of cytotoxicity is an important effector mechanism in the development of HSK. Our results demonstrated that HSV-1-induced keratitis is significantly re-

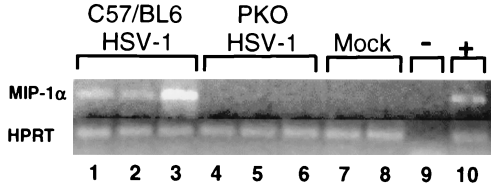


FIG. 7. Detection of MIP-1α mRNA by RT-PCR in the corneas of HSV-1-infected wild-type and PKO mice at 23 days p.i. Expression of mRNA for MIP-1α in the cornea was examined by RT-PCR for HSV-1-infected wild-type and PKO mice, as well as for mock-infected wild-type and PKO mice. Normalized corneal cDNA from each mouse was amplified by PCR using primers for HPRT and MIP-1α. The MIP-1α PCR product (364 bp) and the HPRT PCR product (182 bp) were visualized by agarose gel electrophoresis and ethidium bromide staining. Lanes: 1 to 3, RT-PCR product from the corneas of HSV-1-infected wild-type mice at 23 days p.i. (C57/BL6 HSV-1); 4 to 6, RT-PCR product from the corneas of HSV-1-infected PKO mice at 23 days p.i. (PKO HSV-1); 7; RT-PCR product from the corneas of a mock-infected wildtype mouse; 8, RT-PCR product from the corneas of a mock-infected PKO mouse; 9, negative control, consisting of PCR run without cDNA (−); 10; positive control, consisting of the RT-PCR product from activated macrophages (+). In lanes 1 to 8, each lane contains the RT-PCR product from the corneas of a single mouse.

duced in PKO mice. Compared to wild-type mice, PKO mice had significantly less severe clinical disease following corneal infection with HSV-1. Histopathologic examinations confirmed that the corneas of PKO mice were less extensively infiltrated with inflammatory cells and blood vessels. The difference in corneal thickness measurements between infected wild-type and PKO mice at 23 days p.i. provides further evidence for reduced inflammation in HSV-1-infected PKO mice. PKO mice given an adoptive transfer of T-cell-enriched splenocytes from HSV-1-immune wild-type donors developed HSK similar in severity and time course to that seen in wild-type mice following infection with HSV-1.

The adoptive transfer experiments showed that the reduced disease development seen in HSV-1 infected PKO mice is due to a perforin deficiency in the effector cells that mediate the immunopathology. PKO mice contain all the cells and components of the immune system of wild-type mice except perforin (27, 28). The reconstituted HSV-1-infected PKO mice differed from the nonreconstituted virus-infected PKO mice only by the addition of HSV-1-immune wild-type splenocytes. These results suggest that the decreased susceptibility to HSV-1-induced corneal inflammation in PKO mice is due to a lack of effector cell-mediated cytotoxicity via the perforin pathway. The Fas-FasL pathway of cytotoxicity apparently does not play an important role in the development of HSK, since *gld* mice, which have a null-function mutation in the *fasL* gene, developed clinical and histologic lesions of similar severity to those in wild-type mice upon HSV-1 infection.

$CD8^+$ T cells, NK cells, and $CD4^+$ T cells can mediate cytotoxicity via the perforin mechanism. $CD8^+$ T cells and NK cells have been traditionally thought to be the cells that mediate cytotoxicity via the perforin pathway (28, 53); however, a number of laboratories have recently shown, in viral, tumor, and transplantation models, that $CD4^+$ T cells can mediate cytotoxicity via the perforin-dependent mechanism (4, 15, 26, 33, 40, 46, 47, 51, 61, 67, 68, 70–74). Activation of $CD4^+$-T cell-mediated perforin cytotoxicity was shown to occur most efficiently in the absence of $CD8^+$ T cells (68). Therefore, it appears that any one of these effector cell types is capable of initiating cytotoxicity via the perforin pathway. Each of these cell types has been shown to be able to mediate keratitis in a mouse model following inoculation with HSV-1 (6, 11, 12, 21, 23, 25, 31, 43, 44). Our data show that the presence of perforin in effector lymphocytes is critical in initiation and production of keratitis following intracorneal HSV-1 infection.

An explanation of the role of perforin in keratitis development should take into account the idea that perforin has no known chemotactic function. A plausible model to explain our findings and those of others is that cytotoxicity via the perforin pathway is a key step in initiating keratitis. Any of several different cell types including $CD8^+$ T cells, $CD4^+$ T cells, and NK cells could mediate perforin-dependent cytotoxicity against HSV-1-infected target cells. Perforin-mediated lysis of infected corneal cells may result in the release of cytokines and chemokines such as MIP-1α. This could lead to the influx of macrophages and neutrophils, which are present in the histopathologic lesions of HSK. The inflammatory cells could then amplify the response, possibly through the release of more cytokines and chemokines (16, 57, 59, 60). This amplification phase is consistent with the elevated chemokine expression seen in the cornea during the onset and clinical phases of HSK (55, 57, 59, 60). A similar model invoking cytotoxicity followed by cytokine and chemokine release has been proposed for B3 coxsackievirus-induced myocarditis (16) and contact hypersensitivity (29).

Cytokines and chemokines including interleukin-1β (IL-1β), IL-6, monocyte chemotactic protein 1 (MCP-1), MIP-1α, and MIP-2 are detectable in corneas of mice following HSV-1 infection (55, 57, 59, 60). In vitro studies in mice and humans have shown that MIP-2, KC, IL-6, IL-1β, and IL-8 are produced by HSV-1-infected corneal cultures; this suggests that corneal cells can produce cytokines and chemokines after infection with HSV-1 (45, 57, 69). Inflammatory cells have also been suggested as a source of the elevated levels of MIP-1α which were detected in HSV-1-induced keratitis (57, 60). In another model of virus-induced inflammatory disease (B3 coxsackievirus-induced myocarditis), the levels of MIP-1α were elevated in wild-type mice compared to PKO mice (16).

The importance of MIP-1α in the pathogenesis of HSK has been previously demonstrated in a MIP-1α-deficient mouse model (60). We wanted to examine whether there is a possible mechanistic relationship between perforin and MIP-1α in our murine model of HSK. Our RT-PCR results demonstrated that the difference in the severity of clinical and histologic disease between wild-type and PKO mice was reflected by differences in the presence of MIP-1α in the cornea. The absence of detectable MIP-1α mRNA in the corneas of infected PKO mice in our studies is consistent with the reduced inflammatory-cell infiltration into the corneas of these mice. However, it cannot be determined from our results whether the absence of detectable MIP-1α in the infected PKO mice was caused by a lack of inflammatory cells that may secrete MIP-1α or by the impaired release of MIP-1α due to the absence of perforin-mediated cell lysis. Experiments to examine the relationship between cytotoxicity and the release of chemoattractants are in progress. The role of a panel of cytokines and chemokines, including MIP-1α, which have been implicated in the development of HSK will be examined in detail in PKO and wild-type mice.

It should be pointed out that mechanisms other than those discussed above for the production of keratitis may exist. Even though HSK was significantly reduced in PKO mice compared to wild-type mice in our experiments, it was not completely eliminated. PKO mice were still capable of developing a much reduced form of the keratitis lesion.

In contrast to our findings, a recent study using HSV-1 strain McKrae found no difference in corneal scarring between wild-type and PKO mice following intracorneal infection with HSV-1 (17). These investigators used a different strain and dose of HSV-1 from those used in the experiments in the present study. Following intracorneal inoculation with HSV-1 in mice, rabbits, and guinea pigs, the incidence and severity of keratitis vary with different strains of virus (18, 64–66). The spectrum of disease can vary from mild or nonexistent to severe (18, 64–66). The dose of a particular strain of virus can also affect the incidence of disease (8, 64). In the experiments of Ghiasi et al. (17), HSV-1 McKrae at a dose of $2 \times 10^6$ PFU per eye was used to intracorneally inoculate wild-type and PKO mice. These mice were monitored for corneal disease. The severity of corneal disease was low for both groups ($0.6 \pm 0.3$ and $0.6 \pm 0.2$, respectively, on a scale of 0 through 4). It would be difficult to measure a significant decrease in the severity or incidence of HSV-1-induced corneal disease in PKO mice if the level of disease in wild-type mice was already low. The difference in the results of Ghiasi et al. (17) and our own may be due to a difference in the combination of dose and strain of HSV-1 used in the respective experiments.

We found no difference in the ability of PKO and wild-type mice to clear virus from the eyes. A possible explanation for this finding is that perforin-mediated cytotoxicity may not play an important role in clearing HSV-1 from the eyes. Studies of

hepatitis B virus (19) have shown that virus clearance can occur without cell lysis. Moreover, it has been shown that rotaviruses can be cleared without the involvement of gamma interferon, perforin or FasL (14). A recent study indicated that alpha and beta interferons may play a dominant role in the clearance of HSV-1 in a mouse model (32).

In conclusion, we have shown in a mouse model of HSV-1-induced keratitis that perforin is important in the pathogenesis of corneal inflammation. Perforin-mediated target cell killing may result in the release of cytokines and/or chemokines, which recruit inflammatory cells to the cornea. Inflammatory cells such as neutrophils could then mediate direct tissue damage. A precise understanding of the role of perforin in HSK will require further experiments.

## ACKNOWLEDGMENTS

We thank Robert Myers and Mike Thomas for technical assistance; Lawrence Butcher, Brandon Reinbold, and James Warner for help with the mice; and Jim Thorne for help with statistics.

This study was supported by grants from the National Institutes of Health (RO1-EY11855 and KO2-AI01552) to W.J.M.

## REFERENCES

1. **Allison, J., and A. Strasser.** 1998. Mechanisms of cell death in diabetes: a minor role for CD95. Proc. Natl. Acad. Sci. USA **95:**13818–13822.
2. **Babu, J. S., S. Kanangat, and B. T. Rouse.** 1995. T cell cytokine mRNA expression during the course of the immunopathologic ocular disease herpetic stromal keratitis. J. Immunol. **154:**4822–4829.
3. **Babu, J. S., J. Thomas, S. Kanangat, L. A. Morrison, D. Knipe, and B. T. Rouse.** 1996. Viral replication is required for induction of ocular immunopathology by herpes simplex virus. J. Virol. **70:**101–107.
4. **Blazar, B. R., P. A. Taylor, and D. A. Vallera.** 1997. $CD4^+$ and $CD8^+$ T cells each can utilize a perforin-dependent pathway to mediate lethal graft versus host disease in major histocompatibility complex disparate recipients. Transplantation **64:**571–576.
5. **Bouley, D. M., S. Kanangat, and B. T. Rouse.** 1995. Characterization of herpes simplex virus type-1 infection and herpetic stromal keratitis development in IFN-gamma knockout mice. J. Immunol. **155:**3964–3971.
6. **Bouley, D. M., S. Kanangat, and B. T. Rouse.** 1996. The role of the innate immune system in the reconstituted SCID mouse model of herpetic stromal keratitis. Clin. Immunol. Immunopathol. **80:**23–30.
7. **Brandt, C. R., L. Coakley, and D. R. Grau.** 1992. A murine model of herpes simplex virus-induced ocular disease for antiviral drug testing. J. Virol. Methods **36:**209–222.
8. **Deshpande, S. P., M. Zheng, M. Dahesia, and B. T. Rouse.** 2000. Pathogenesis of herpes simplex virus induced ocular inflammatory lesions in B-cell-deficient mice. J. Virol. **74:**3517–3524.
9. **DiPrieto, L., M. Burdick, G. Low, S. L. Kunkel, and A. Strieler.** 1998. MIP-1 alpha as a critical macrophage chemoattractant in murine wound healing. J. Clin. Investig. **101:**1693–1698.
10. **Doymaz, M., and B. T. Rouse.** 1991. MHC II-restricted, $CD4^+$ cytotoxic T lymphocytes specific for herpes simplex virus-1: implications for the development of herpetic stromal keratitis in mice. Clin. Immunol. Immunopathol. **61:**398–409.
11. **Doymaz, M., and B. T. Rouse.** 1992. Immunopathology of herpes simpex virus infections. Curr. Top. Microbiol. Immunol. **179:**121–136.
12. **Doymaz, M., and B. T. Rouse.** 1992. Herpetic stomal keratitis: an immunopathologic disease mediated by $CD4^+$ T lymphocytes. Investig. Ophthalmol. Visual Sci. **33:**2165–2173.
13. **Foster, C. S., Y. Tsai, J. Monroe, R. Campbell, M. Cestari, R. Wetzig, D. Knipe, and M. I. Greene.** 1986. Genetic studies on murine susceptibility to herpes simplex keratitis. Clin. Immunol. Immunopathol **40:**313–325.
14. **Franco, M. A., C. Tin, L. Rott, J. VanCott, J. McGhee, and H. Greenberg.** 1997. Evidence for $CD8^+$ T cell immunity to murine rotavirus in the absence of perforin, Fas, and gamma interferon. J. Virol. **71:**479–486.
15. **Gagnon, S. J., F. Ennis, and A. L. Rothman.** 1999. Bystander target cell lysis and cytokine production by dengue virus-specific human $CD4^+$ cytotoxic T lymphocyte clones. J. Virol. **73:**3623–3629.
16. **Gebhard, J., C. M. Perry, S. Harkins, T. Lane, I. Mena, V. Asensio, I. L. Campbell, and J. L. Whitton.** 1998. Coxackievirus B3-induced myocarditis: perforin exacerbates disease, but plays no detectable role in virus clearance. Am. J. Pathol. **153:**417–428.
17. **Ghiasi, H., S. Cai, G. Perng, A. Nesburn, and S. L. Wechsler.** 1999. Perforin pathway is essential for protection of mice against lethal ocular HSV-1 challenge but not corneal scarring. Virus Res. **65:**97–101.
18. **Grau, D. R., R. Visalli, and C. R. Brandt.** 1989. Herpes simplex virus stromal keratitis is not titer-dependent and does not correlate with neurovirulence. Investig. Ophthalmol. Visual Sci. **30:**2774–2780.
19. **Guidotti, L., T. Ishikawa, M. V. Hobbs, B. Matzke, R. Screiber, and F. Chisari.** 1996. Intracellular inactivation of the hepatitis B virus by cytotoxic T lymphocytes. Immunity **4:**25–36.
20. **Hendricks, R. L.** 1997. An immunologist's view of herpes simplex keratitis. Cornea **16:**503–506.
21. **Hendricks, R. L., and T. M. Tumpey.** 1990. Contribution of virus and immune factors to herpes simplex virus type 1 induced corneal pathology. Investig. Ophthalmol. Visual Sci. **31:**29–39.
22. **Hendricks, R. L., and T. M. Tumpey.** 1991. Concurrent regeneration of T lymphocytes and susceptibility to HSV-1 corneal stromal disease. Curr. Eye Res. **10**(Suppl.)**:**47–53.
23. **Hendricks, R. L., M. Tao, and J. C. Glorioso.** 1989. Alteration in the antigenic stucture of two major HSV-1 glycoproteins influence immune regulation and susceptibility to murine herpes keratitis. J. Immunol. **142:**263–269.
24. **Hendricks, R. L., T. M. Tumpey, and A. Finnegan.** 1992. IFN-gamma and IL-2 are protective in the skin but pathologic in the corneas of HSV-1 infected mice. J. Immunol. **149:**3023–3028.
25. **Hendricks, R. L., M. Janowicz, and T. M. Tumpey.** 1992. Critical role of Langerhans' cells in $CD4^+$-mediated, but not $CD8^+$-mediated, immunopathology in HSV-1 infected mouse corneas. J. Immunol. **148:**2522–2529.
26. **Hishii, M., J. Kurnick, T. Ramirez, and F. Pandolfi.** 1999. Studies of the mechanism of cytolysis by tumour-infiltrating lymphocytes. Clin. Exp. Immunol. **116:**388–394.
27. **Kagi, D., B. Ledermann, D. Burki, P. Seiler, B. Odematt, E. Podack, R. M. Zinkernagel, and H. Hengartner.** 1994. Cytotoxicity mediated by T cells and natural killer cells is greatly impaired in perforin-deficient mice. Nature **369:**31–36.
28. **Kagi, D., B. Ledermann, K. Burki, R. M. Zinkernagel, and H. Hengartner.** 1996. Moleular mechanisms of lymphocyte-mediated cytotoxicity and their role in immunological protection and pathogenesis in vivo. Annu. Rev. Immunol. **14:**207–232.
29. **Kehren, J., C. Desvignes, M. Drasteva, M. Ducluzeau, M. Hahne, D. Kagi, and J. F. Nicolas.** 1999. Cytotoxicity is mandatory for $CD8^+$ T cell-mediated contact hypersensitivity. J. Exp. Med. **189:**779–786.
30. **Kojima, H., N. Shinohara, S. Hanaoka, T. Saitoh, T. Katayama, H. Yagita, F. Alt, A. Matsuzawa, and H. Takayama.** 1994. Two distinct pathways of specific killing revealed by perforin mutant cytotoxic T lymphocytes. Immunity **1:**357–364.
31. **Ksander, B., and R. L. Hendricks.** 1987. Cell mediated immune tolerance to HSV-1 antigens associated with reduced susceptibility to HSV-1 corneal lesions. Investig. Ophthalmol. Visual Sci. **28:**1986–1993.
32. **Leib, D. A., T. Harrison, K. M. Laslo, M. Machalek, N. J. Moorman, and H. W. Virgin.** 1999. Interferons regulate the phenotype of wildtype and mutant herpes simplex viruses in vivo. J. Exp. Med. **189:**663–672.
33. **Lewinsohn D. M., T. Bement, J. C. Xu, D. Lynch, K. H. Grabstein, and M. Alderson.** 1998. Human purified protein derivative-specific $CD4^+$ T cells use both CD95-dependent and CD95-independent cytolytic mechanisms. J. Immunol. **160:**2374–2379.
34. **Lin, M. T., S. A. Strohlman, and D. Hinton.** 1997. Mouse hepatitis virus is cleared from the central nervous systems of mice lacking perforin-mediated cytolysis. J. Virol. **71:**383–391.
35. **Lowin, B., F. Beermann, A. Schmidt, and J. Tschopp.** 1994. A null mutation in the perforin gene impairs cytolytic T lymphocyte and natural killer cell-mediated cytotoxicity. Proc. Natl. Acad. Sci. USA **91:**11571–11575.
36. **Maggs, D. J., E. Chang, M. P. Nasisse, and W. J. Mitchell.** 1998. Persistence of herpes simplex virus type 1 DNA in chronic conjunctival and eyelid lesions of mice. J. Virol. **72:**9166–9172.
37. **Mercadal, C. M., D. Bouley, D. DeStephano, and B. T. Rouse.** 1993. Herpetic stromal keratitis in the reconstituted *scid* mouse model. J. Virol. **67:**3404–3408.
38. **Metcalf, J. F., D. Hamilton, and R. Reichert.** 1979. Herpetic keratitis in athymic nude mice. Infect. Immun. **26:**1164–1171.
39. **Metcalf, J. F., and B. A. Michaelis.** 1984. Herpetic keratitis in inbred mice. Investig. Ophthalmol. Visual Sci. **25:**1222–1225.
40. **Miskovsky, E., A. Liu, W. Pavlat, R. Viveen, P. Stanhope, D. Finzi, W. Fox, and R. Siliciano.** 1994. Studies of the mechanism of cytolysis by HIV-I specific $CD4^+$ human CTL clones induced by candidate AIDS vaccines. J. Immunol. **153:**2787–2799.
41. **Mitchell, W. J., R. DeSanto, S. Zhang, W. Odenwald, and H. Arnheiter.** 1993. Herpes simplex virus pathogenesis in transgenic mice is altered by the homeodomain protein Hox 1.3. J. Virol. **67:**4484–4491.
42. **Mitchell, W. J., P. Gressens, J. Martin, and R. DeSanto.** 1994. Herpes simplex virus type 1 DNA persistence, progressive disease and transgenic immediate early gene promoter activity in chronic corneal infections in mice. J. Gen. Virol. **75:**1201–1210.
43. **Newell, C. K., S. Martin, D. Sendele, C. M. Mercadal, and B. T. Rouse.** 1989. Role of T lymphocytes in the pathogenesis of herpetic stromal keratitis. J. Virol. **63:**769–775.
44. **Niemialtowski, M., and B. T. Rouse.** 1992. Predominance of Th1 cells in

ocular tissues during herpetic stromal keratitis. J. Immunol. **149:**3035–3039.
45. **Oakes, J. E., C. Monteiro, C. Cubitt, and R. Lausch.** 1993. Induction of interleukin-8 gene expression is associated with herpes simplex virus infection of human corneal keratocytes but not human corneal epithelial cells. J. Virol. **67:**4777–4784.
46. **Ohminami, H., M. Yasukawa, S. Kaneko, Y. Abe, Y. Ishida, and S. Fujita.** 1999. Fas-independent and nonapoptotic cytotoxicity mediated by a human $CD4^+$ T cell clone directed against an acute myelogenous leukemia associated DEK-CAN fusion peptide. Blood **93:**925–935.
47. **Rivoltini, L., M. Radrizzani, P. Accornero, F. Belli, M. Colombo, and G. Parmiani.** 1998. Human melanoma-reactive $CD4^+$ and $CD8^+$ CTL clones resist Fas ligand induced apoptosis and use Fas/Fas ligand independent mechanisms for tumor killing. J. Immunol. **161:**1220–1230.
48. **Rouse, B. T.** 1996. Virus-induced immunopathologies. Adv. Virus Res. **47:** 353–376.
49. **Russell, R., M. P. Nasisse, H. Larsen, and B. T. Rouse.** 1984. Role of T lymphocytes in the pathogenesis of herpetic stromal keratitis. Investig. Ophthalmol. Visual Sci. **25:**938–944.
50. **Sabelko-Downes, K., A. H. Cross, and J. H. Russell.** 1999. Dual role for Fas ligand in the initiation of and recovery from experimental allergic encephalomyelitis. J. Exp. Med. **189:**1195–1205.
51. **Schnyder, B., K. Frutig, A. Limat, and W. Pichler.** 1998. T cell mediated cytotoxicity against keratinocytes in sulfamethoxazole induced skin reaction. Clin. Exp. Allergy **28:**1412–1417.
52. **Severson, C. D., D. Berg, D. E. LaFrenz, and T. Feldbush.** 1987. An alternative method of panning for rat B lymphocytes. Immunol. Lett. **15:**291–295.
53. **Shresta, S. C. T. Pham, D. Thomas, T. Graubert, and T. J. Ley.** 1998. How do cytotoxic lymphocytes kill their targets? Curr. Opin. Immunol. **10:**581–87.
54. **Streilein, J. W., M. Dana, and B. R. Ksander.** 1998. Immunity causing blindness: five different paths to herpes stromal keratitis. Immunol. Today **18:**443–449.
55. **Su, Y. H., X. T. Yan, J. Oakes, and R. Lausch.** 1996. Protective antibody therapy is associated with reduced chemokine transcripts in herpes simplex virus type 1 corneal infection. J. Virol. **70:**1277–1281.
56. **Tang, H., G. C. Sharpe, K. Chen, and H. Braley-Mullen.** 1998. Kinetics of cytokine gene expression in thyroids of mice developing granulomatous experimental autoimmune thyroiditis. J. Autoimmun. **11:**581–589.
57. **Thomas, J., S. Kanangat, and B. T. Rouse.** 1998. Herpes simplex virus replication-induced expression of chemokines and proinflammatory cytokines in the eye: implications in herpetic stromal keratitis. J. Interferon Cytokine Res. **18:**681–690.
58. **Thomas, J., and B. T. Rouse.** 1998. Immunopathology of herpetic stromal keratitis: discordance in $CD4^+$ T cell function between euthymic host and reconstituted SCID recipients. J. Immunol. **160:**3965–3970.
59. **Tumpey, T. M., H. Cheng, X. T. Yan, J. Oakes, and R. Lausch.** 1998. Chemokine synthesis in the HSV-1 infected cornea and its suppression by interleukin-10. J. Leukoc. Biol. **63:**486–492.
60. **Tumpey, T. M., H. Cheng, D. Cook, O. Smithies, J. Oakes, and R. N. Lausch.** 1998. Absence of macrophage inflammatory protein 1 alpha prevents the development of blinding herpes stromal keratitis. J. Virol. **72:**3705–3710.
61. **Vergelli, M., B. Hemmer, P. Muraro, L. Tranquilli, W. Biddison, and R. Martin.** 1997. Human autoreactive $CD4^+$ T cell clones use perforin or Fas/Fas ligand mediated pathways for target cell lysis. J. Immunol. **158:**2756–2761.
62. **Waldner, H., R. Sobel, E. Howard, and V. K. Kuchroo.** 1997. Fas- and FasL-deficient mice are resistant to the induction of autoimmune encephalomyelitis. J. Immunol. **159:**3100–3103.
63. **Walsh, C. M., M. Maltoubian, C. Liu, R. Ueda, J. Young, R. Ahmed, and W. R. Clark.** 1994. Immune function in mice lacking the perforin gene. Proc. Natl. Acad. Sci. USA **91:**10854–10858.
64. **Wander, A. H., Y. Centifanto, and H. E. Kaufman.** 1980. Strain specificity of clinical isolates of herpes simplex virus. Arch. Ophthalmol. **98:**1458–1461.
65. **Wander, A. H., H. C. Bubel, and S. G. McDowell.** 1987. The pathogenesis of herpetic ocular disease in the guinea pig. Arch. Virol. **95:**197–209.
66. **Williams, L. E., A. Nesburn, and H. E. Kaufman.** 1965. Experimental induction of disciform keratitis. Arch. Ophthalmol. **73:**112–114.
67. **Williams, N. S., and V. H. Engelhard.** 1996. Identification of a population of $CD4^+$ CTL that utilizes a perforin rather than a Fas ligand dependent cytotoxic mechanism. J. Immunol. **156:**153–159.
68. **Williams, N. S., and V. H. Engelhard.** 1997. Perforin-dependent cytotoxic activity and lymphokine secretion by $CD4^+$ T cells are regulated by $CD8^+$ T cells. J. Immunol. **159:**2091–2099.
69. **Yan, X. T., T. M. Tumpey, S. Kunkel, J. Oakes, and R. Lausch.** 1998. Role of MIP-2 in neutrophil migration and tissue injury in the herpes simplex virus-1 infected cornea. Investig. Ophthalmol. Visual Sci. **39:**1854–1862.
70. **Yasukawa, M., A. Inatsuki, T. Horiuchi, and Y. Kobayashi.** 1991. Functional heterogeneity among herpes simplex virus-specific human $CD4^+$ T cells. J. Immunol. **146:**1341–1347.
71. **Yasukawa, M., Y. Yakushijin, H. Asegawa, M. Miyake, Y. Hitsumoto, S. Kimura, N. Takeuchi, and S. Fujita.** 1993. Expression of perforin and membrane-bound lymphotoxin in virus-specific $CD4^+$ human cytotoxic T cell clones. Blood **81:**1527–1534.
72. **Yasukawa, M., Y. Yakushijin, and S. Fujita.** 1996. Two distinct mechanisms of cytotoxicity mediated by herpes simplex virus-specific $CD4^+$ human cytotoxic T cell clones. Clin. Immunol. Immunopathol. **78:**70–76.
73. **Yasukawa, M., H. Ohminami, Y. Yakushijin, J. Arai, A. Hasegawa, Y. Ishida, and S. Fujita.** 1999. Fas-independent cytotoxicity mediated by human $CD4^+$ CTL directed against herpes simplex virus infected cells. J. Immunol. **162:** 6100–6106.
74. **Yasukawa, M., H. Ohminami, J. Arai, Y. Kasahara, Y. Ishida, and S. Fujita.** 2000. Granule exocytosis and not the Fas/Fas ligand system is the main pathway of cytotoxicity mediated by alloantigen-specific $CD4^+$ as well as $CD8^+$ cytotoxic T lymphocytes in humans. Blood **95:**2352–2355.